Clinical Cancer Research

Circulating Cell-Free miR-375 as Surrogate Marker of Tumor Burden in Merkel Cell Carcinoma

Kaiji Fan[1,2,3,4], Cathrin Ritter[2,3,4], Paul Nghiem[5], Astrid Blom[5], Monique E. Verhaegen[6], Andrzej Dlugosz[6], Niels Ødum[7], Anders Woetmann[7], Richard W. Tothill[8,9], Rodney J. Hicks[9,10], Michael Sand[11], David Schrama[12], Dirk Schadendorf[3,13], Selma Ugurel[13], and Jürgen C. Becker[2,3,4,13]

Abstract

Purpose: Merkel cell carcinoma (MCC) is an aggressive skin cancer with neuroendocrine differentiation. There is an unmet need for MCC-specific blood-based surrogate biomarkers of tumor burden; circulating cell-free miRNA may serve this purpose.

Experimental Design: Expression of miR-375 was quantified in 24 MCC and 23 non-MCC cell lines, 67 MCC and 58 non-MCC tumor tissues, sera of 2 preclinical MCC models, and sera of 109 patients with MCC and 30 healthy controls by nCounter human-v2-miRNA expression or miR-375–specific real-time PCR assays. The patients' sera consisted of two retrospective (discovery and training) and two prospective (validation) cohorts.

Results: miR-375 expression was high in MCC cell lines and tissues compared with non-MCCs. It was readily detected in MCC-conditioned medium and sera of preclinical models bearing MCC xenografts. miR-375 levels were higher in sera from tumor-bearing patients with MCC than in tumor-free patients or healthy controls ($P < 0.0005$). Moreover, miR-375 serum levels correlated with tumor stage in tumor-bearing ($P = 0.037$) but not in tumor-free ($P = 0.372$) patients with MCC. miR-375 serum level showed high diagnostic accuracy to discriminate tumor-bearing and tumor-free patients with MCC as demonstrated by ROC curve analysis in the retrospective cohorts (AUC = 0.954 and 0.800) as well as in the prospective cohorts (AUC = 0.929 and 0.959). miR-375 serum level reflected dynamic changes in tumor burden of patients with MCC during therapeutic interventions.

Conclusions: Circulating cell-free miR-375 proved as a surrogate marker for tumor burden in MCC without restriction to polyomavirus positivity; it thus appears to be useful for therapy monitoring and the follow-up of patients with MCC.
Clin Cancer Res; 24(23); 5873–82. ©2018 AACR.

Introduction

The knowledge and understanding of the biology and immunology of Merkel cell carcinoma (MCC), a highly aggressive skin cancer with neuroendocrine features, expanded dramatically over the past decade, allowing new therapeutic interventions for this previously untreatable cancer (1). MCC carcinogenesis can be initiated either by the clonal integration of the Merkel cell polyomavirus (MCPyV) into the host cell genome or by UV-mediated DNA damage. Either mechanism fosters the striking immunogenicity of MCC explaining the strong therapeutic effect of immune checkpoint inhibitors. Inhibitors of the PD-1/PD-L1 checkpoint axis have been demonstrated to result in durable tumor responses (2–4). Notably, the highest efficacy was observed in first-line therapy of patients with limited tumor burden, stressing the need for reliable approaches for early detection of tumor recurrence in patients with MCC who are tumor free after surgery (2–4). Furthermore, 40% to 60% of cases do not respond to checkpoint inhibition (2). Thus, a blood-based surrogate biomarker of tumor burden, which can be serially assessed, could be a helpful tool for both early detection of disease relapse and monitoring of treatment.

The American Joint Committee on Cancer (AJCC) incorporated several blood-based biomarkers into their staging systems, for example, prostate-specific antigen for prostate cancer (5), or α-fetoprotein and β-HCG for testicular cancer (6). Unfortunately, for the majority of solid tumors, no reliable blood-based biomarkers have yet been established. Advances in genomic technologies have identified numbers of candidate markers based on circulating cell-free (cf) DNA and RNA (7, 8). Although cancer in general is associated with increased serum DNA concentrations, most approaches using circulating cf DNA rely on tumor-specific DNA mutations, such as EGFR mutations in non–small cell lung

[1]Department of Dermatology, Medical University of Graz, Graz, Austria. [2]Department of Translational Skin Cancer Research, University Hospital Essen, Essen, Germany. [3]German Cancer Consortium (DKTK), Essen, Germany. [4]German Cancer Research Center (DKFZ), Heidelberg, Germany. [5]Department of Dermatology/Medicine, University of Washington, Seattle, Washington. [6]Department of Dermatology, University of Michigan, Ann Arbor, Michigan. [7]Department of Immunology and Microbiology, University of Copenhagen, Copenhagen, Denmark. [8]Centre for Cancer Research, University of Melbourne, Melbourne, Australia. [9]Peter MacCallum Cancer Centre, Melbourne, Australia. [10]Sir Peter MacCallum Department of Oncology, University of Melbourne, Melbourne, Australia. [11]Department of Dermatology, Ruhr-University Bochum, Bochum, Germany. [12]Department of Dermatology, University Hospital Würzburg, Würzburg, Germany. [13]Department of Dermatology, University Hospital Essen, Essen, Germany.

Note: Supplementary data for this article are available at Clinical Cancer Research Online (http://clincancerres.aacrjournals.org/).

Corresponding Author: Jürgen C. Becker, Department of Translational Skin Cancer Research, Universitätsstrasse 1, S05 T05 B, Essen 45141, Germany. Phone: +49-201-1836727; Fax: +49-201-1836945; E-mail: j.becker@dkfz.de

doi: 10.1158/1078-0432.CCR-18-1184

Translational Relevance

The introduction of new therapies for advanced Merkel cell carcinoma being effective in approximately half of the patients created the need for blood-based surrogate biomarkers of tumor burden. Currently, serum reactivity to Merkel cell polyomavirus is used for this purpose, but is restricted to virus-positive tumors only. Here, we demonstrate that circulating cell-free miR-375 discriminates tumor-bearing and tumor-free patients in four independent cohorts from Australia, Europe, and the United States. Moreover, repeated quantification of miR-375 during therapeutic interventions showed a precise reflection of the dynamic change in tumor burden in correlation to radiologic imaging. Our data indicate that serum miR-375 may serve as a surrogate marker of tumor burden in patients with MCC regardless of their virus status, and may be particularly useful in therapy monitoring.

cancer (9, 10) or BRAF mutations in melanoma (11). Because of the absence of specific hotspot mutations, this strategy is not applicable for MCC.

An alternative approach takes advantage of cf miRNAs specifically overexpressed in certain cancer types (12). Because miRNAs may be actively released from cancer cells and are highly resistant to degradation, sera and/or plasma from patients with cancer contain large amounts of miRNAs derived from tumor cells (12). Indeed, cf miRNAs have already been recognized as biomarkers for a variety of different cancer entities, for example, miR-1290 in colorectal cancer (13) or a miRNA panel in breast cancer (14). In this study, we describe the abundant expression and release of miR-375 in MCC tissues and MCC cell lines, respectively, and demonstrate miR-375 serum levels as a valid surrogate biomarker of tumor burden in patients with MCC. This approach is potentially useful both for detection of early recurrence and monitoring response to therapy.

Materials and Methods

Patients and clinical samples

For tumor-tissue analysis, formalin-fixed and paraffin-embedded (FFPE) samples from 67 MCCs, 48 melanomas, and 10 basal cell carcinomas were used. For serum analysis, a total of 438 serum samples from 139 individuals were used (30 healthy subjects and 109 patients with MCC including two retrospectively selected and two prospectively collected patients sample cohorts; Fig. 1). The patient cohorts and corresponding serum samples were collected at the Medical University of Graz (Graz, Austria), University of Washington/Seattle (Seattle, WA), University Hospital Essen (Essen, Germany), and University of Melbourne (Melbourne, Australia). Patients' characteristics are given in Supplementary Tables S3 to S6. Serum samples were generated from peripheral blood draws and cryopreserved following established SOPs (15). The study was conducted in accordance with ethical guideline provided in the "Declaration of Helsinki." The investigational protocol was approved by the Institutional Review Board/Ethic Committee (17-7539-BO; Ethics Committee of the University Duisburg-Essen, and sharing of de-identified samples was approved by the ethics committees in Graz, Melbourne, and Seattle). Informed consent was obtained from all individual participants prior to analyses.

Cell lines

The MCC and non-MCC cell lines have been described before in Supplementary Tables S1 and S2.

NanoString nCounter analysis

miRNA expression in MCC cell lines was analyzed using the nCounter Human v2 miRNA Expression Assay Kit (NanoString) according to the manufacturer's instructions. Data were extracted using the nCounter RCC collector and analyzed in nSolver Analysis Software.

miRNA *in situ* hybridization

Six-micron thick sections of FFPE tumor samples were used for miRNA *in situ* hybridization. In brief, slides were deparaffinized and placed in Tecan Freedom Evo–automated hybridization instrument (Tecan), using a previously described protocol (16). Double-FAM–labeled miR-375 and scramble LNA probes (both at 40 nmol/L; Exiqon) were applied for hybridization at 57°C for 60 minutes. All slides were dehydrated and then mounted with Eukitt medium (Electron Microscopy Sciences).

qRT-PCR for miRNA

Applied Biosystems TaqMan MicroRNA assays (Thermo Fisher Scientific) were applied to measure the respective miRNAs according to the manufacturer's instructions. Predesigned TaqMan microRNA assays for miR-182 (ID002334), miR-106b (ID000442), miR-19b (ID000396), miR-200c (ID002300), and miR-375 (ID000564) were used. The quantification cycle threshold (C_q) values of target miRNAs were normalized to the small nucleolar RNA RNU6B (ID001093) or the spiked-in cel-miR-39 as indicated and relative expression to the respective comparator was calculated using the $2^{-\Delta\Delta C_q}$ method.

Preclinical *in vivo* models

For chicken chorioallantoic membrane (CAM) experiments, 2×10^6 MCC cells in 50 μL culture medium were mixed 1:1 in Matrigel (BD Biosciences) and placed on the CAM at day 9 postfertilization. For murine xenotransplantation experiments, tumors were induced by subcutaneous injection of 5×10^6 cells in 50 μL mixed 1:1 with Matrigel into the lateral flank of 6-week-old female NOD.CB17-Prkdcscid/J mice (Charles River Laboratories) housed under specific pathogen-free conditions (17). Approximately 100 μL of chicken or mouse blood was collected 4 days or 28 days, respectively, after MCC cell grafting and centrifuged at 3,000 rpm for 10 minutes at 4°C. The obtained supernatant was centrifuged again at 12,000 rpm for 15 minutes to remove all remaining debris. Animal studies were approved by the Austrian Ministry of Education and Science (BMWF-66.010/0151-II/3b/2012).

PET/CT imaging

PET/CT studies were performed on the Discovery LS PET/CT scanner (GE Medical Systems) and the image acquisition protocol was as described previously (18). Order-subset estimate maximization algorithm was applied to reconstruct images using iterative reconstruction (18). Disease burden was determined using a

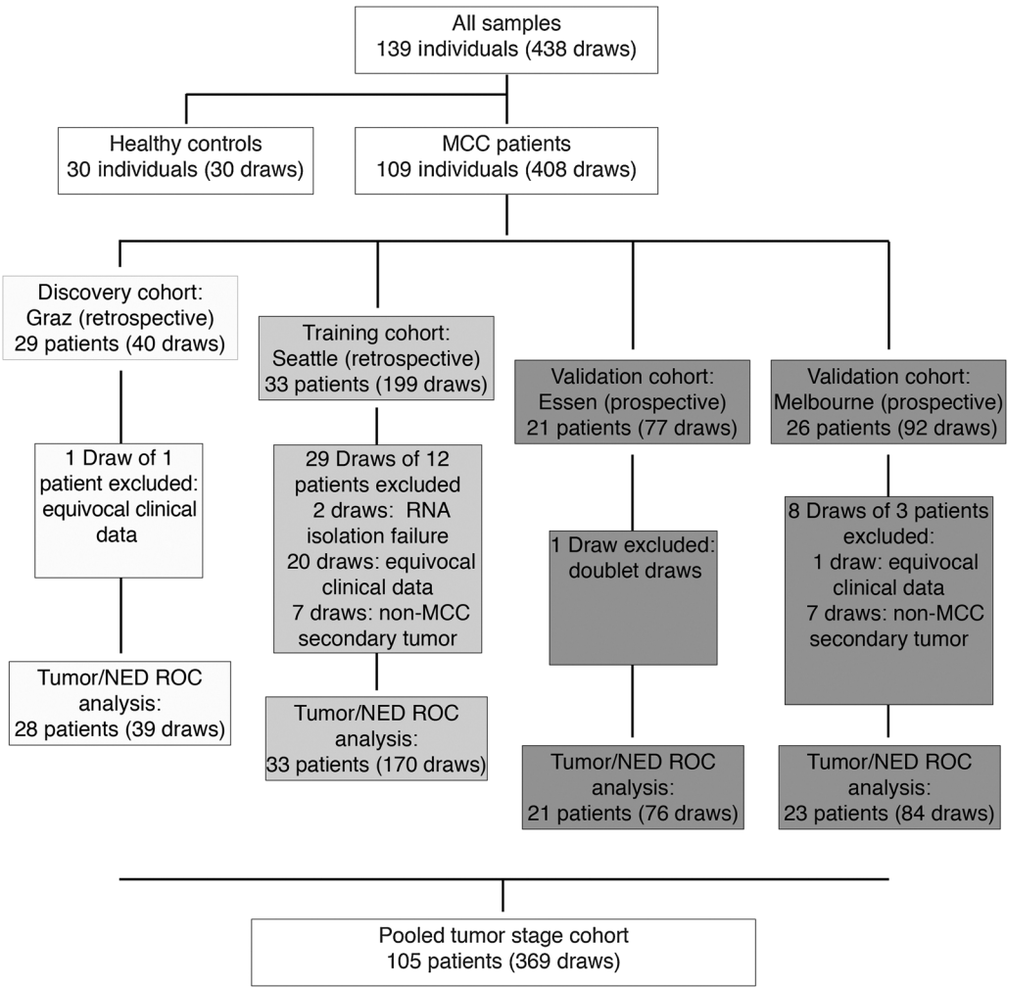

Figure 1.
Study flow diagram of serum analysis for circulating cf miR-375, including two retrospective and two prospective MCC patient cohorts.

segmentation algorithm based on lesion intensity with operator interaction to exclude regions of nonpathologic uptake (MIM Encore, MIM Software Inc.) and was expressed as a metabolic tumor volume (MTV).

Statistical analysis

Statistical analyses were performed using GraphPad Prism 6.0 Software (GraphPad Software Inc.) and R studio. Experiments containing two groups were analyzed using Mann–Whitney *U* test. Experiments containing more than two groups were analyzed using Kruskal–Wallis test, an unpaired nonparametric ANOVA. R studio was applied in statistical analysis as indicated: "heatmap2" in gplots R package for differentiated expression of miRNAs; pROC R package for ROC curve analysis (19); and ggpubr R package for correlation analysis. A P value smaller than 0.05 was considered significant; the respective P values are indicated in the figures as follows: *, $P < 0.05$; **, $P < 0.01$; ***, $P < 0.001$. ROC curve analysis was performed for each cohort independently; all four cohorts were combined to determine the correlation between cf miR-375 level and MCC tumor staging.

Results

miR-375 is highly expressed in MCC cell lines and tissues

The nCounter Human v2 miRNA expression assay (NanoString Technology) was performed in six well-established classical MCC cell lines demonstrating miR-375 as one of the most abundant miRNAs in all MCC cell lines (Fig. 2A). This strong expression of miR-375 in MCC was further substantiated in a larger panel of 21 classical MCC cell lines by real-time PCR (Fig. 2B; Supplementary Table S1). miR-375 expression was independent of the viral status of the MCC cell lines, that is, both MCPyV-positive and -negative cell lines showed high levels of miR-375 (Fig. 2B). However, none of the three variants, MCPyV-negative MCC cell lines, which are characterized by an adherent growth pattern expressed comparable amounts of miR-375 (Fig. 2B; Supplementary Table S1). It is important to note that the representativeness of these variant MCC cell lines for MCC is controversially discussed (1, 20). Next, the high expression of miR-375 was confirmed in 67 MCC tumor lesions by qRT-PCR (Fig. 2C). Again, miR-375 expression was largely independent of the MCPyV status. In contrast, miR-375

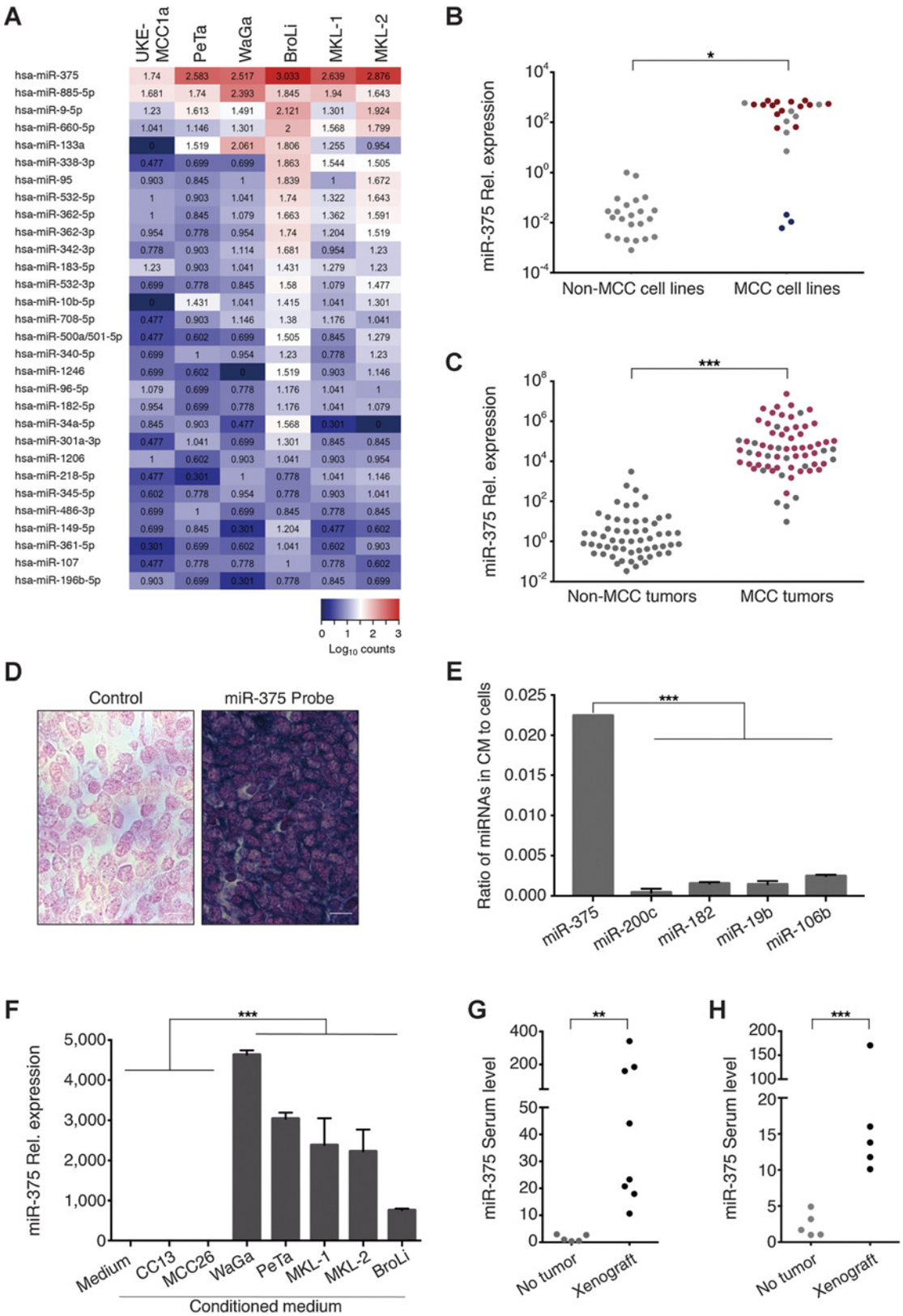

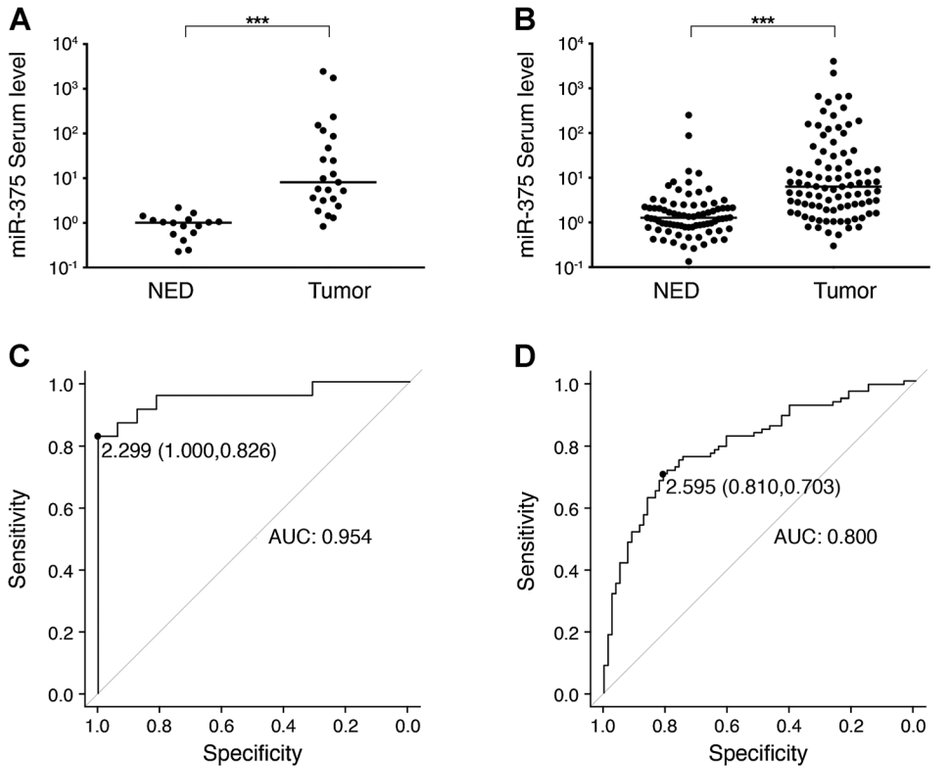

Figure 3.

Circulating cf miR-375 in serum discriminates patients with MCC with and without presence of disease: the retrospective discovery and training cohorts. **A** and **B,** cf miR-375 in sera of patients with MCC was determined by qRT-PCR in duplicate, and normalized to spiked-in cel-mir-39. Values were calculated relative to the serum of a patient with MCC with no evidence of disease (Graz cohort) by the $2^{-\Delta\Delta C_q}$ method. Results are depicted in Cleveland dot plots categorized in patients with no (NED) or with evidence of disease. **C** and **D,** ROC curves showing the sensitivity and specificity of miR-375 serum levels to discriminate tumor-bearing versus NED patients. The AUC, optimal cut-off values and their sensitivity and specificity are given. **A** and **C,** Graz cohort; **B** and **D,** Seattle cohort. Patients' characteristics are given in Supplementary Tables S3 and S4. The horizontal line indicates the median, Mann–Whitney *U* test and pROC R were performed as described in Statistical analysis (***, $P < 0.001$).

expression was low in 23 non-MCC skin cancer cell lines and 58 non-MCC skin cancer tissues (Fig. 2B and C; Supplementary Table S2). miRNA *in situ* hybridization demonstrated high expression levels of miR-375 in MCC tissue (Fig. 2D).

Presence of circulating cf miR-375 in MCC-conditioned medium and serum of MCC xenograft-bearing preclinical models

Extracellular miRNAs may serve as means of communication between cells over short and long distances (21). In line with this notion, circulating cf miRNA has been detected in serum and plasma of patients with cancer (22). Thus, we next tested whether miR-375 was also present as extracellular miRNA in cell culture supernatants of the miR-375–expressing MCC cell lines. Notably, although all miRNAs abundantly expressed in MCC cells, that is, miR-375, miR-200c, miR-182, miR-19b, and miR-106b, were detectable in MCC-conditioned medium, miR-375 demonstrated by far the highest ratio of extracellular to cellular miRNA (Fig. 2E; Supplementary Fig. S1). The presence of extracellular miR-375 in MCC-conditioned medium was confirmed in a larger series of classical MCC cell lines (Fig. 2F). As expected from the lack of miR-375 expression in the variant MCC cell lines MCC13 and MCC26, the conditioned media did not contain this miRNA. Next, we translated the *in vitro* findings into an *in vivo* setting taking advantage of two recently established preclinical models for MCC. To this end, WaGa cells were xenografted either on the CAM of chicken embryos ($n = 8$, Fig. 2G) or into the flank of NOD.CB17-Prkdc^{scid}/J mice ($n = 5$, Fig. 2H). In both models, circulating cf

Figure 2.

The highly expressed miR-375 in MCC cell lines and tissues is also present as cf miRNA in MCC-conditioned media as well as in sera of MCC-bearing preclinical models. **A,** Heatmap depicting the relative expression of the 30 most abundant miRNAs in six MCC cell lines. Data obtained by nCounter Human v2 miRNA Expression Assay (NanoString Technology). **B,** miR-375 expression in 24 MCC cell lines [21 classical MCPyV positive ($n = 14$, red) or negative ($n = 7$, gray), and three variant MCC cell lines (blue); details in Supplementary Table S1] as well as 23 non-MCC skin cancer (melanoma and squamous cell carcinoma), lung cancer, kidney, and fibroblast cell lines (details in Supplementary Table S2) was quantified by qRT-PCR in triplicates. The relative expression of miR-375 was normalized to U6 and is depicted relative to 293T cells as calculated by the $2^{-\Delta\Delta C_q}$ method. **C,** miR-375 expression in 58 non-MCC skin cancer tissue samples (48 melanomas and 10 basal cell carcinomas) as well as 67 MCC tissue samples [49 MCPyV positive (red) and 18 MCPyV negative (gray)] was determined by qRT-PCR in triplicate. The expression level of miR-375 was normalized to U6 and is depicted relative to one randomly selected melanoma sample as calculated by the$2^{-\Delta\Delta C_q}$ method. **D,** *In situ* hybridization (ISH) for miR-375 in a representative MCC tissue. Intense miR-375 ISH signal (right), and background staining for the scrambled control (left). Scale bar, 10 μm. **E,** The presence of miR-375, miR-200c, miR-182, miR-19b, and miR-106b in 200 μL of conditioned medium from the MCC cell line WaGa (48-hour culture of 106 cells/mL) and in the cells themselves was determined by qRT-PCR in triplicate. The ratio of respective miRNA calculated by the $2^{-\Delta\Delta C_q}$ method in conditioned medium to the cells is depicted. **F,** miR-375 presence in conditioned medium from seven different MCC cell lines was determined in triplicate. The expression level of miR-375 was normalized to spiked-in cel-mir-39 and is depicted relative to MCC13-conditioned medium as calculated by the $2^{-\Delta\Delta C_q}$ method. **G,** Circulating cf miR-375 in sera of chicken embryos bearing 4-day-old xenotransplants of WaGa MCC cells on the chorioallantoic membrane was determined by qRT-PCR in triplicate. The expression level of miR-375 was normalized to spiked-in cel-mir-39 and is depicted relative to the serum of an untreated chicken embryo as calculated by the $2^{-\Delta\Delta C_q}$ method. **H,** cf miR-375 in sera of NOD.CB17-Prkdcscid/J mice with or without subcutaneous WaGa MCC xenografts was determined by qRT-PCR in triplicate. The expression level of miR-375 was normalized to spiked-in cel-mir-39 and is depicted relative to the sera of tumor-free NOD.CB17-Prkdcscid/J control mice as calculated by the $2^{-\Delta\Delta C_q}$ method. Mann–Whitney *U* test was performed as described in Statistical analysis (*, $P < 0.05$; **, $P < 0.005$; ***, $P < 0.001$).

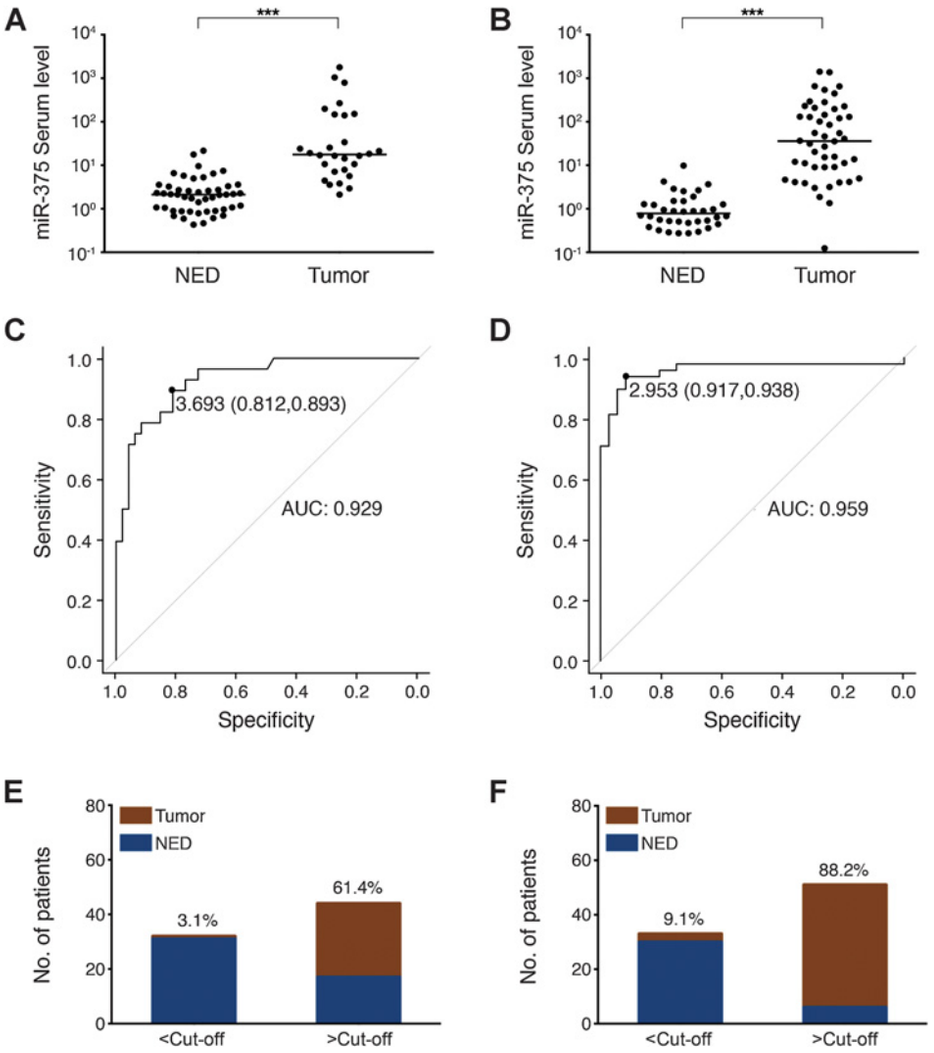

Figure 4.
Circulating cf miR-375 in serum discriminates patients with MCC with and without presence of disease: the prospective validation cohorts. **A** and **B,** cf miR-375 in sera of patients with MCC was determined by qRT-PCR in duplicate, and normalized to spiked-in cel-mir-39. Values were calculated relative to the serum of a patient with MCC with no evidence of disease (Graz cohort) by the $2^{-\Delta\Delta C_q}$ method. Results are depicted in Cleveland dot plots categorized in patients with no (NED) or with evidence of disease. **C** and **D,** ROC curves showing the sensitivity and specificity of miR-375 serum levels to discriminate tumor-bearing versus NED patients. The AUC, optimal cut-off values and their sensitivity and specificity are given. **E** and **F,** The mean optimal miR-375 serum level cutoff was calculated from the optimal cut-off values of the retrospective discovery and validation cohorts as 2.42. Proportions of patients with MCC of the prospective cohorts with (brown) or without (blue) tumor burden below or above this mean optimal cutoff are depicted. Percentages of patients with MCC with tumor burden within each group are given. **A**, **C**, and **E,** Essen cohort. **B**, **D**, and **F,** Melbourne cohort. Patients' characteristics are given in Supplementary Tables S3 and S4. The horizontal line indicates the median, Mann–Whitney *U* test and pROC R were performed as described in Statistical analysis (*, $P < 0.05$; **, $P < 0.005$; ***, $P < 0.001$).

miR-375 was detected at substantially higher levels in the sera of xenograft-bearing animals compared with tumor-free control animals.

Circulating cf miR-375 serum levels differentiate patients with MCC with or without evidence of disease

Prompted by these encouraging preclinical results, we next measured the presence of circulating cf miR-375 in sera of patients with MCC utilizing the same real-time PCR-based assay (study flow according to REMARK provided in Fig. 1). In the discovery cohort, we analyzed 40 serum samples retrospectively selected from cryoconserved sera drawn from 29 MCC patients' measurable disease or with no evidence of disease (NED). As depicted in Fig. 3A, serum levels of circulating cf miR-375 were significantly higher in patients with measurable disease as compared with patients with NED ($P < 0.001$, Mann–Whitney *U* test). ROC curve analysis was performed by plotting the sensitivity against the specificity for different thresholds of circulating cf miR-375 to discriminate between tumor-bearing and tumor-free patients. This analysis demonstrated a miR-375 serum level of 2.299 as optimal cut off with a specificity of 1.000 and a sensitivity of 0.826 resulting in an AUC of 0.954 with a 95% confidence interval (CI) of 0.89 to 1.00 (Fig. 3C).

We next analyzed a training cohort of 199 serum samples obtained from 33 patients with MCC over the course of their disease, revealing that serum cf miR-375 levels were significantly higher in patients with MCC with measurable disease as compared with NED patients ($P < 0.001$, Mann–Whitney *U* test; Fig. 3B). ROC curve analysis demonstrated a miR-375 serum level of 2.595 as optimal cutoff with a specificity of 0.810 and a sensitivity of 0.703 resulting in an AUC of 0.800 (95% CI, 0.73–0.86; Fig. 3D).

For validation, we analyzed two prospectively collected serum cohorts from Essen (77 serum samples from 21 patients with MCC) and Melbourne (92 serum samples from 26 patients with MCC). In both cohorts, serum cf miR-375 levels were significantly higher in patients with MCC with measurable disease as compared with NED patients ($P < 0.001$, Mann–Whitney *U* test; Fig. 4A and B). ROC curve analysis revealed a miR-375 serum level of 3.693 as optimal cutoff with a specificity of 0.812 and a sensitivity of 0.893, resulting in an AUC of 0.929 (95% CI, 0.87–0.98; Fig. 4C) for the Essen cohort, and a miR-375 serum level of

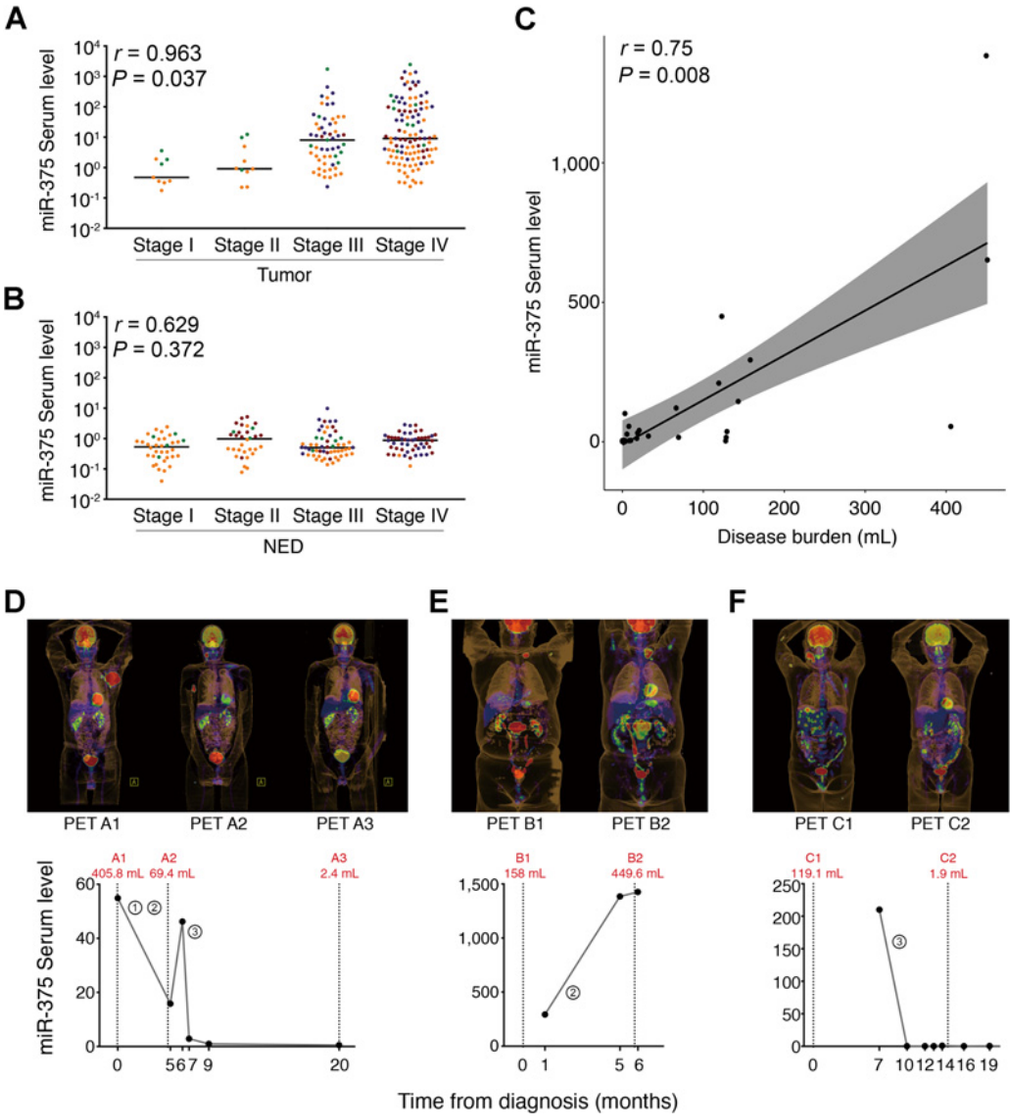

Figure 5.

Circulating cf miR-375 serum levels correlate with disease stage and tumor burden of patients with MCC. cf miR-375 in sera of patients with MCC was determined by qRT-PCR in duplicate, and normalized to spiked-in cel-mir-39. Values were calculated relative to the serum of a patient with MCC with no evidence of disease (Graz cohort) by the 2-$\Delta\Delta C_q$ method. **A** and **B,** Results are depicted in Cleveland dot plots combined for all four cohorts categorized by AJCC stage at the time of blood draw for patients with (**A**) or without (**B**) evidence of disease; to discern from which cohorts the samples were derived, the data points were color-coded: Graz, green; Seattle, yellow; Essen, dark red; Melbourne, purple. Correlation analysis between cf miR-375 serum levels and MCC tumor stages was performed in R using the "ggpubr" package; the horizontal line indicates the median. **C,** Correlation analysis for cf miR-375 serum level and MCC tumor burden as quantified by PET/CT scan for the Melbourne cohort was performed in R using the "ggpubr" package. **D–F,** cf miR-375 serum levels are plotted over the course of disease together with the tumor volume, which was calculated from PET/CT scans depicted above the respective graphs for three exemplary patients from the Melbourne cohort (**D:** p_#16, **E:** p_#6, and **F:** p_#10). The numbers circled indicate the different therapies: ① radiotherapy, ② chemotherapy, and ③ immunotherapy. The clinical course of patient **D** is described in Results; patient **E** showed disease progression during chemotherapy; patient **F** showed a complete response to checkpoint inhibition.

2.953 as optimal cutoff with a specificity of 0.917 and a sensitivity of 0.938 resulting in an AUC of 0.959 (95% CI, 0.91–1.00; Fig. 4D) for the Melbourne cohort.

The mean of the optimal cut-off values for serum miR-375 of the retrospective discovery and training cohorts was calculated as 2.42. When this mean cut-off value (2.42) as well as respective percentiles (increasing quartiles: 25th = 1.00, 50th = 2.32, 75th = 8.16, and 90th = 100.0) of cf miR-375 serum level calculated from the retrospective cohorts were applied to distinguish tumor-bearing and tumor-free patients in the two prospective validation cohorts, the tumor-bearing patients rate with miR-375 serum level below versus above this value were 3.1% versus 61.4% in the Essen cohort (Fig. 4E) and 9.1% versus 88.2% in the Melbourne cohort (Fig. 4F). These results were confirmed when calculating the respective percentiles for the prospective cohorts (Supplementary Fig. S3). Furthermore, combined miR-375 serum data from

30 healthy donors and all patients with MCC demonstrated that circulating cf miR-375 levels were significantly higher in patients with MCC with measurable disease as compared with the healthy donors ($P < 0.001$, Mann–Whitney *U* test; Supplementary Fig. S2). It should be noted, however, that in some of the patients with NED, the miR-375 level was even lower than in the control patients. This observation may be caused by secondary diseases such as type II diabetes mellitus in the control group or by the administered therapies in the NED group (e.g., radiation, immune, or chemotherapy; refs. 23, 24). Thus, the dynamics of miR-375 in sequential serum samples of patients with MCC appears to be more informative than single samples.

Circulating cf serum miR-375 correlates with the disease stage in tumor-bearing patients with MCC

To further assess the informative value of circulating cf miR-375, we next asked whether the serum level could discriminate different disease stages of MCC in tumor-bearing patients. To address the challenge of limited cohort sizes in this rare disease (Supplementary Fig. S4), we pooled all four patient cohorts for this analysis; the respective cohorts were color coded. Indeed, there was a significant correlation of circulating cf miR-375 serum levels and AJCC stage at the time of the blood draw for patients with measurable disease (Fig. 5A; $P = 0.037$, ggpubr R), but not for patients with NED at the time of blood draw (Fig. 5B; $P = 0.372$, ggpubr R). Moreover, based on the exact MTV assessment performed by PET/CT scans within the Melbourne cohort, we found a significant correlation between the cf miR-375 serum level and MCC tumor volume ($P = 0.008$, $r = 0.75$, ggpubr R; Fig. 5C).

Circulating cf serum miR-375 allows MCC disease course monitoring

Availability of effective therapeutic options for advanced metastatic MCC emphasizes the need for closely monitoring treatment responses. The serum kinetics, that is, the short half-life, of miRNA allowed serum levels of circulating cf miR-375 to be used to track dynamic changes of MCC tumor burden during therapy (25). As depicted in Fig. 5D–F, serum levels of miR-375 were strongly correlated with metabolic tumor volume during the course of therapy. For example, one patient with MCC (Fig. 5D) with a large bulky tumor (405.8 mL) presented with a high serum level of cf miR-375 (54.9), which decreased during radiochemotherapy to 15.8 in parallel with shrinkage of MTV on PET/CT (69.4 mL). When the patient's tumor progressed at 6 months following the onset of treatment, the cf miR-375 serum level rose accordingly (46.2). The patient subsequently received immune checkpoint inhibition therapy leading to an almost complete response with MTV reduction to 2.4 mL, reflected by a decrease in miR-375 serum level to 0.52. This strong correlation between MCC tumor volume and amounts of circulating cf miR-375 could be confirmed in multiple patients from whom serum samples were collected sequentially over time (Fig. 5E and F; Supplementary Fig. S5).

Discussion

Until recently, there was no effective treatment for metastatic MCC that was not amenable to surgery and/or radiation. With the advent of immune-modulating therapies based on checkpoint-inhibiting antibodies, this situation has changed dramatically (2–4). However, not all patients respond to therapy and acquired resistance is an additional problem. Notably, although first-line treatment results in objective responses in almost 2 of 3 of patients, response decreases to 1 of 3 in the second-line setting (3, 4). Thus, it appears that the efficient treatment of patients with MCC relies on the early detection of recurrence and/or progression, which can be difficult using standard tissue biopsy techniques. Imaging approaches are relatively costly and involve small but documented risks (26). Blood-based biomarkers as a surrogate of tumor burden would be advantageous, because the non-invasive nature of these "liquid biopsies" allows them to be repeatedly applied to monitor the patient's clinical course over time, providing guidance on when imaging might be helpful in localizing disease (27). Moreover, they integrated information on disease burden without the need to know exactly where it may have arisen.

Different approaches have been investigated to establish an MCC-specific blood-based biomarker. Although neuron-specific enolase (NSE) and chromogranin A (CGA) are reliable biomarkers for some neuroendocrine tumors like small-cell lung cancer (SCLC; ref. 28), neither NSE nor CGA was effective to distinguish between patients with MCC with or without tumor burden (29). On the basis of the strong association of MCC with MCPyV, antibodies against MCPyV-encoded oncoproteins, that is, the transforming early genes, were tested for their use as surrogate markers for active MCC disease (30–32). Indeed, antibody titers correlated with tumor burden as they cleared in patients during remission and reoccurred at high titers in the case of recurrence. Consequently, the NCCN guidelines list oncoprotein antibodies as a legitimate and useful approach to follow-up patients with MCC. To this end, the ROC analysis demonstrated very similar results when antibodies to MCPyV oncoproteins and miR-375 serum levels were established in the same samples (Supplementary Fig. S6). Notably, however, patients with UV-associated MCPyV-negative MCCs produce no antibodies to MCPyV oncoproteins, so that in such patients, the miR-375 approach would currently be the only applicable surrogate marker of tumor burden. Moreover, oncoprotein antibodies are not useful in an ongoing way for patients who do not produce these antibodies at baseline even if suffering from virus-associated MCC, which constitute about half of the patients. Thus, if no baseline draw is done, it is impossible later to determine whether the patient initially produced antibodies at the time of diagnosis (32).

miR-375 was initially described as a pancreas-specific miRNA regulating insulin secretion and pancreatic islet development (33). Soon thereafter, aberrant miR-375 expression was detected in prostate cancer (34), lung cancer with neuroendocrine differentiation (35), and MCC (36, 37). Consistent with these reports, we here confirmed the strong expression of miR-375 in MCC *in vitro*, *in vivo*, and *in situ* in the largest series reported to date. Notably, miR-375 was consistently overexpressed in both virus- and UV-associated (i.e., virus negative) MCC. Furthermore, in contrast to other miRNAs abundant in MCC cells (miR-200c, miR-19b, miR-182, and miR-106b), miR-375 was the only one detected at substantial levels as extracellular miRNA. This latter finding can be explained by the known function of miR-375 as an exosomal shuttle miRNA participating in the active genetic exchange between cells (38). Indeed, we found evidence that miR-375 is enriched in the exosomal fraction derived from the conditioned media (data not shown). Because miR-375 is not present in circulating blood cells (39), that is, it is not expressed in

lymphocytes, red blood cells, or platelets (40), comparison of miRNA spectrums between serum and plasma revealed that miR-375 is not differentially expressed (41).

In summary, based on the abundant expression of miR-375 in MCC cell lines and tissues, and its extracellular presence in MCC cell culture supernatants as well as sera of tumor-bearing preclinical animal models, we suspected and subsequently demonstrated cf miR-375 can serve as a surrogate marker of tumor burden to follow patients with MCC. Notably, our results indicate that cf miR-375 not only discriminates patients with or without evidence of disease, but also correlates with the burden of disease and can be a useful tool to monitor the response to therapy and thus may allow a more aimed indication of PET/CT imaging. An appropriate next step will be to validate the use of miR-375 as a surrogate marker of MCC tumor burden in patient samples serially collected as part of clinical trials that are increasingly being carried out for MCC.

Disclosure of Potential Conflicts of Interest

S. Ugurel reports receiving other commercial research support from Bristol-Myers Squibb and MerckSerono, and is a consultant/advisory board member for Bristol-Myers Squibb, Merck Sharp and Dohme, and Roche. J.C. Becker reports receiving speakers bureau honoraria from Amgen, Bristol-Myers Squibb, and MerckSerono, and is a consultant/advisory board member for eTheRNA, MerckSerono, and Sanofi. N. Ødum is a consultant/advisory board member for Mindera Inc. No potential conflicts of interest were disclosed by the other authors.

Authors' Contributions

Conception and design: K. Fan, C. Ritter, R.J. Hicks, J.C. Becker
Development of methodology: K. Fan, C. Ritter, P. Nghiem, A. Dlugosz, N. Ødum, J.C. Becker
Acquisition of data (provided animals, acquired and managed patients, provided facilities, etc.): C. Ritter, P. Nghiem, A. Blom, M.E. Verhaegen, N. Ødum, R.W. Tothill, R.J. Hicks, D. Schrama, D. Schadendorf, S. Ugurel, J.C. Becker
Analysis and interpretation of data (e.g., statistical analysis, biostatistics, computational analysis): K. Fan, A. Woetmann, R.J. Hicks, M. Sand, D. Schrama, J.C. Becker
Writing, review, and/or revision of the manuscript: K. Fan, C. Ritter, P. Nghiem, A. Blom, M.E. Verhaegen, N. Ødum, A. Woetmann, R.W. Tothill, R.J. Hicks, M. Sand, D. Schrama, D. Schadendorf, S. Ugurel, J.C. Becker
Administrative, technical, or material support (i.e., reporting or organizing data, constructing databases): P. Nghiem, A. Dlugosz, R.W. Tothill, S. Ugurel, J.C. Becker
Study supervision: J.C. Becker

Acknowledgments

This work was part of the FP7 project IMMOMEC funded by the European Commission, including funding for K. Fan. K. Fan was supported by the graduate program DK MOLIN of the Austrian FWF. P. Nghiem and A. Blom were supported by K24-; P30 CA015704. M.E. Verhaegen and A. Dlugosz were supported by NIH grants CA183084 and CA189352. R.J. Hicks is supported by NHMRC Practitioner Fellowship APP1108050. The authors like to express their appreciation to Jeanette Raleigh, Athena Hatzimihalis, and Jason Callahan from the Peter MacCallum Cancer Centre, Melbourne, Australia as well as Lisa Zimmer, Elisabeth Livingston, and Bastian Schilling from the University Hospital Essen, Germany, for the clinical evaluation of patients.

The costs of publication of this article were defrayed in part by the payment of page charges. This article must therefore be hereby marked *advertisement* in accordance with 18 U.S.C. Section 1734 solely to indicate this fact.

Received April 18, 2018; revised June 15, 2018; accepted July 24, 2018; published first July 30, 2018.

References

1. Becker JC, Stang A, DeCaprio JA, Cerroni L, Lebbe C, Veness M, et al. Merkel cell carcinoma. Nat Rev Dis Primers 2017;3:17077.
2. Terheyden P, Becker JC. New developments in the biology and the treatment of metastatic Merkel cell carcinoma. Curr Opin Oncol 2017;13: 1263–79.
3. Kaufman HL, Russell J, Hamid O, Bhatia S, Terheyden P, D'Angelo SP, et al. Avelumab in patients with chemotherapy-refractory metastatic Merkel cell carcinoma: a multicentre, single-group, open-label, phase 2 trial. Lancet Oncol 2016;17:1374–85.
4. Nghiem PT, Bhatia S, Lipson EJ, Kudchadkar RR, Miller NJ, Annamalai L, et al. PD-1 blockade with pembrolizumab in advanced merkel-cell carcinoma. N Engl J Med 2016;374:2542–52.
5. Salman JW, Schoots IG, Carlsson SV, Jenster G, Roobol MJ. Prostate specific antigen as a tumor marker in prostate cancer: biochemical and clinical aspects. Adv Exp Med Biol 2015;867:93–114.
6. Sturgeon CM, Duffy MJ, Stenman UH, Lilja H, Brunner N, Chan DW, et al. National Academy of Clinical Biochemistry laboratory medicine practice guidelines for use of tumor markers in testicular, prostate, colorectal, breast, and ovarian cancers. Clin Chem 2008;54:e11–79.
7. Wan JCM, Massie C, Garcia-Corbacho J, Mouliere F, Brenton JD, Caldas C, et al. Liquid biopsies come of age: towards implementation of circulating tumour DNA. Nat Rev Cancer 2017;17:223–38.
8. Lee JH, Long GV, Boyd S, Lo S, Menzies AM, Tembe V, et al. Circulating tumour DNA predicts response to anti-PD1 antibodies in metastatic melanoma. Ann Oncol 2017;28:1130–6.
9. Goldman JW, Noor ZS, Remon J, Besse B, Rosenfeld N. Are liquid biopsies a surrogate for tissue EGFR testing? Ann Oncol 2018;29:i38–i46.
10. Knebel F, Bettoni F, Shimada A, Cruz M, Alessi JV, Negrao M, et al. Sequential liquid biopsies reveal dynamic alterations of EGFR driver mutations and indicate EGFR amplification as a new mechanism of resistance to osimertinib in NSCLC. Clin Cancer Res 2018;24:67.
11. Santiago-Walker A, Gagnon R, Mazumdar J, Casey M, Long GV, Schadendorf D, et al. Correlation of BRAF mutation status in circulating-free dna and tumor and association with clinical outcome across four BRAFi and MEKi clinical trials. Clin Cancer Res 2016;22: 567–74.
12. Mitchell PS, Parkin RK, Kroh EM, Fritz BR, Wyman SK, Pogosova-Agadjanyan EL, et al. Circulating microRNAs as stable blood-based markers for cancer detection. Proc Natl Acad Sci U S A 2008;105:10513–8.
13. Imaoka H, Toiyama Y, Fujikawa H, Hiro J, Saigusa S, Tanaka K, et al. Circulating microRNA-1290 as a novel diagnostic and prognostic biomarker in human colorectal cancer. Ann Oncol 2016;27:1879–86.
14. Chan M, Liaw CS, Ji SM, Tan HH, Wong CY, Thike AA, et al. Identification of circulating microRNA signatures for breast cancer detection. Clin Cancer Res 2013;19:4477–87.
15. Tuck MK, Chan DW, Chia D, Godwin AK, Grizzle WE, Krueger KE, et al. Standard operating procedures for serum and plasma collection: early detection research network consensus statement standard operating procedure integration working group. J Proteome Res 2009;8:113–7.
16. Lindahl LM, Fredholm S, Joseph C, Nielsen BS, Jonson L, Willerslev-Olsen A, et al. STAT5 induces miR-21 expression in cutaneous T cell lymphoma. Oncotarget 2016;7:45730–44.
17. Willmes C, Adam C, Alb M, Volkert L, Houben R, Becker JC, et al. Type I and II IFNs inhibit Merkel cell carcinoma via modulation of the Merkel cell polyomavirus T antigens. Cancer Res 2012;72:2120–8.
18. Bayne M, Hicks RJ, Everitt S, Fimmell N, Ball D, Reynolds J, et al. Reproducibility of "intelligent" contouring of gross tumor volume in non-small-cell lung cancer on PET/CT images using a standardized visual method. Int J Radiat Oncol Biol Phys 2010;77:1151–7.
19. Robin X, Turck N, Hainard A, Tiberti N, Lisacek F, Sanchez JC, et al. pROC: an open-source package for R and S+ to analyze and compare ROC curves. BMC Bioinformatics 2011;12:77.

20. Daily K, Coxon A, Williams JS, Lee CC, Coit DG, Busam KJ, et al. Assessment of cancer cell line representativeness using microarrays for Merkel cell carcinoma. J Invest Dermatol 2015;135:1138–46.
21. Xu L, Yang BF, Ai J. MicroRNA transport: a new way in cell communication. J Cell Physiol 2013;228:1713–9.
22. Mahn R, Heukamp LC, Rogenhofer S, von Ruecker A, Muller SC, Ellinger J. Circulating microRNAs (miRNA) in serum of patients with prostate cancer. Urology 2011;77:1265.
23. Diener Y, Walenda T, Jost E, Brummendorf TH, Bosio A, Wagner W, et al. MicroRNA expression profiles of serum from patients before and after chemotherapy. Genom Data 2015;6:125–7.
24. Higuchi C, Nakatsuka A, Eguchi J, Teshigawara S, Kanzaki M, Katayama A, et al. Identification of circulating miR-101, miR-375 and miR-802 as biomarkers for type 2 diabetes. Metabolism 2015;64:489–97.
25. Gong J, Wu Y, Zhang X, Liao Y, Sibanda VL, Liu W, et al. Comprehensive analysis of human small RNA sequencing data provides insights into expression profiles and miRNA editing. RNA Biol 2014;11:1375–85.
26. Huntington SF, Svoboda J, Doshi JA. Cost-effectiveness analysis of routine surveillance imaging of patients with diffuse large B-cell lymphoma in first remission. J Clin Oncol 2015;33:1467–74.
27. Wong SQ, Tothill RW, Dawson S-J, Hicks RJ. Wet or dry? Do liquid biopsy techniques compete with or complement pet for disease monitoring in oncology? J Nucl Med 2017;58:869–70.
28. Isgro MA, Bottoni P, Scatena R. Neuron-specific enolase as a biomarker: biochemical and clinical aspects. Adv Exp Med Biol 2015;867:125–43.
29. Gaiser MR, Daily K, Hoffmann J, Brune M, Enk A, Brownell I. Evaluating blood levels of neuron specific enolase, chromogranin A, and circulating tumor cells as Merkel cell carcinoma biomarkers. Oncotarget 2015;6: 26472–82.
30. Paulson KG, Carter JJ, Johnson LG, Cahill KW, Iyer JG, Schrama D, et al. Antibodies to merkel cell polyomavirus T antigen oncoproteins reflect tumor burden in merkel cell carcinoma patients. Cancer Res 2010;70: 8388–97.
31. Touzé A, Le Bidre E, Laude H, Fleury MJ, Cazal R, Arnold F, et al. High levels of antibodies against merkel cell polyomavirus identify a subset of patients with merkel cell carcinoma with better clinical outcome. J Clin Oncol 2011;29:1612–9.
32. Paulson KG, Lewis CW, Redman MW, Simonson WT, Lisberg A, Ritter D, et al. Viral oncoprotein antibodies as a marker for recurrence of Merkel cell carcinoma: a prospective validation study. Cancer 2017;123: 1464–74.
33. Poy MN, Eliasson L, Krutzfeldt J, Kuwajima S, Ma X, Macdonald PE, et al. A pancreatic islet-specific microRNA regulates insulin secretion. Nature 2004;432:226–30.
34. Wach S, Nolte E, Szczyrba J, Stöhr R, Hartmann A, Ørntoft T, et al. MicroRNA profiles of prostate carcinoma detected by multiplatform microRNA screening. Int J Cancer 2012;130:611–21.
35. Nishikawa E, Osada H, Okazaki Y, Arima C, Tomida S, Tatematsu Y, et al. miR-375 is activated by ASH1 and inhibits YAP1 in a lineage-dependent manner in lung cancer. Cancer Res 2011;71:6165–73.
36. Renwick N, Cekan P, Masry PA, McGeary SE, Miller JB, Hafner M, et al. Multicolor microRNA FISH effectively differentiates tumor types. J Clin Invest 2013;123:2694–702.
37. Abraham KJ, Zhang X, Vidal R, Pare GC, Feilotter HE, Tron VA. Roles for miR-375 in neuroendocrine differentiation and tumor suppression via notch pathway suppression in merkel cell carcinoma. Am J Pathol 2016;186:1025–35.
38. Valadi H, Ekstrom K, Bossios A, Sjostrand M, Lee JJ, Lotvall JO. Exosome-mediated transfer of mRNAs and microRNAs is a novel mechanism of genetic exchange between cells. Nat Cell Biol 2007;9: 654–9.
39. Pritchard CC, Kroh E, Wood B, Arroyo JD, Dougherty KJ, Miyaji MM, et al. Blood cell origin of circulating microRNAs: a cautionary note for cancer biomarker studies. Cancer Prev Res 2012;5:492–7.
40. Mitchell AJ, Gray WD, Hayek SS, Ko YA, Thomas S, Rooney K, et al. Platelets confound the measurement of extracellular miRNA in archived plasma. Sci Rep 2016;6:32651.
41. Wang K, Yuan Y, Cho J-H, McClarty S, Baxter D, Galas DJ. Comparing the microRNA spectrum between serum and plasma. PLoS One 2012;7: e41561.